1521-009X/48/10/861–872$35.00
DRUG METABOLISM AND DISPOSITION

https://doi.org/10.1124/dmd.120.000064
Drug Metab Dispos 48:861–872, October 2020

Comparison of In Vitro to In Vivo Extrapolation Approaches for Predicting Transporter-Mediated Hepatic Uptake Clearance Using Suspended Rat Hepatocytes

Na Li, Akshay Badrinarayanan, Xingwen Li, John Roberts, Mike Hayashi, Manpreet Virk, and Anshul Gupta

Department of Pharmacokinetics and Drug Metabolism, Amgen Research, Amgen Inc., Cambridge, Massachusetts

Received April 3, 2020; accepted July 8, 2020

ABSTRACT

Clearance (CL) prediction remains a significant challenge in drug discovery, especially when complex processes such as drug transporters are involved. The present work explores various in vitro to in vivo extrapolation (IVIVE) approaches to predict hepatic CL driven by uptake transporters in rat. Broadly, two different IVIVE methods using suspended rat hepatocytes were compared: initial uptake CL ($PS_{u,inf}$) and intrinsic metabolic CL ($CL_{int,met}$) corrected by unbound hepatocytes to medium partition coefficient (Kp_{uu}). Kp_{uu} was determined by temperature method (Temp $Kp_{uu,ss}$), homogenization method (Hom $Kp_{uu,ss}$), and initial rate method ($Kp_{uu,v0}$). In addition, the impact of bovine serum albumin (BSA) on each of these methods was investigated. Twelve compounds, which are known substrates of organic anion-transporting polypeptides representing diverse chemical matter, were selected for these studies. As expected, $CL_{int,met}$ alone significantly underestimated hepatic CL for all the test compounds. Overall, predicted hepatic CL using $PS_{u,inf}$ with BSA, Hom $Kp_{uu,ss}$ with BSA, and Temp $Kp_{uu,ss}$ showed the most robust correlation with in vivo rat hepatic CL. Adding BSA improved hepatic CL prediction for selected compounds when using the $PS_{u,inf}$ and Hom $Kp_{uu,ss}$ methods, with minimal impact on the Temp $Kp_{uu,ss}$ and $Kp_{uu,v0}$ methods. None of the IVIVE approaches required an empirical scaling factor. These results suggest that supplementing rat hepatocyte suspension with BSA may be essential in drug discovery research for novel chemical matters to improve CL prediction.

SIGNIFICANCE STATEMENT

The current investigation demonstrates that hepatocyte uptake assay supplemented with 4% bovine serum albumin is a valuable tool for estimating unbound hepatic uptake clearance (CL) and Kp_{uu}. Based upon the extended clearance concept, direct extrapolation from these in vitro parameters significantly improved the overall hepatic CL prediction for organic anion-transporting polypeptide substrates in rat. This study provides a practical in vitro to in vivo extrapolation strategy for predicting transporter-mediated hepatic CL in early drug discovery.

Introduction

Prediction of human pharmacokinetics (PK) of drug candidates is a major focus during drug discovery to reduce attrition during clinical development. Liver is the major organ responsible for drug disposition and elimination. Upon active uptake or passive diffusion from blood into hepatocytes, drugs undergo metabolism and biliary excretion. Therefore, quantitative prediction of hepatic clearance (CL) is an essential step toward accurately predicting human PK. Although allometric scaling across preclinical species has been commonly used for human PK prediction in drug discovery, mechanism-driven in vitro to in vivo extrapolation (IVIVE) is the preferred approach to predict hepatic CL because of the species difference in the function and/or expression of drug metabolizing enzymes and transporters in liver. When metabolism is the predominant CL mechanism, liver microsome or hepatocytes have served as an essential tool for predicting hepatic CL (Kilford et al., 2009; Hallifax et al., 2010; Di et al., 2012). However, when transporters are involved in drug disposition and elimination, the in vitro to in vivo correlation (IVIVC) and human PK prediction become highly uncertain (Shitara et al., 2013). Particularly, when hepatic uptake is the rate-determining step for hepatic CL, direct extrapolation from intrinsic metabolic CL significantly underestimates the drug CL observed in vivo. Due to the differences between the in vitro and in vivo systems (e.g., transporter expression level, activity, static vs. dynamic state), the empirical scaling factor has been proposed to optimize the prediction of hepatic uptake CL (Jones et al., 2012; Li et al., 2014). The empirical

No funding is involved for this work.
https://doi.org/10.1124/dmd.120.000064.
This article has supplemental material available at dmd.aspetjournals.org.

ABBREVIATIONS: AAFE, absolute average fold error; BSA, bovine serum albumin; CHRM, cryopreserved hepatocyte thawing medium; CL, clearance; CL_H, systemic plasma clearance mediated by hepatic elimination; CL_{int}, hepatic intrinsic clearance; $CL_{int,met}$, intrinsic hepatic metabolic clearance; DMEM, Dulbecco's modified Eagle's medium; $f_{u,hep}$, unbound fraction in hepatocyte suspension incubation; $f_{u,KHB\ w\ 4\%,BSA}$, unbound fraction in KHB buffer containing 4% BSA; $f_{u,liver\ tissue}$, unbound fraction in rat liver tissue; $f_{u,p}$, unbound fraction in rat plasma; IVIVC, in vitro to in vivo correlation; IVIVE, in vitro to in vivo extrapolation; KHB, Krebs-Henseleit buffer; Kp, hepatocytes to medium partition coefficient at steady state; $Kp_{uu,ss}$, unbound hepatocytes to medium partitioning coefficient at steady state; LC-MS/MS, liquid chromatography–tandem mass spectrometry; OATP, organic anion-transporting polypeptide; PS_{inf}, hepatic uptake clearance for total drug; $PS_{inf,act}$, hepatic active uptake clearance for total drug; $PS_{inf,dif}$, passive influx for total drug; $PS_{u,inf}$, unbound hepatic uptake clearance; PK, pharmacokinetics; RMSLE, root mean squared logarithmic error.

scaling factor has been found to be system- and compound-dependent, thus presenting a great challenge to implementing this approach in supporting drug discovery efforts.

Quantitative IVIVE approaches have been demonstrated to predict the hepatic CL from uptake CL obtained in cryopreserved human hepatocytes, although these examples are limited to only a few organic anions (Watanabe et al., 2010, 2011). Based upon the extended clearance concept, Izumi et al. (2017) demonstrated improved IVIVE for a variety of drugs by correcting intrinsic metabolic CL with Kp_{uu}. However, for the highly bound compounds, the application of these IVIVE approaches are still limited because of the experimental challenges in accurately determining hepatic uptake CL and Kp_{uu} because of the significant nonspecific binding to the cell surface and experimental devices, and limited analytical sensitivity to accurately determine the unbound fraction in matrices.

In addition to the differences in transporter protein expression and activity, another difference between in vitro systems from in vivo is that in vitro hepatic uptake assay is often carried out in a protein free condition which is in contrast to the systemic circulation where albumin is present under physiological concentrations. Primarily synthesized in liver, albumin is a key protein that maintains the oncotic pressure of blood and has been proven to be involved in drug metabolism and transport (Tessari, 2003; Rabbani and Ahn 2019). For the highly bound compounds, the nonspecific binding to the assay device and/or cell membrane surface could significantly contribute to the inaccuracy or underestimation of in vitro transport rate. The phenomenon of albumin-mediated hepatic uptake has been reported previously in various experimental systems (Tsao et al., 1988a,b). Recent studies have demonstrated that the unbound intrinsic hepatic uptake CL was enhanced by addition of bovine serum albumin (BSA) or human serum albumin, subsequently resulting in improvement in the prediction of the hepatic uptake CL of organic anion-transporting polypeptide (OATP) substrates in rat/human hepatocyte suspension (Miyauchi et al., 2018; Kim et al., 2019).

A robust mechanism-driven IVIVE strategy is pivotal for building confidence in human PK prediction to prioritize compounds during drug discovery phase. Rodent is the most commonly used preclinical species for assessing pharmacokinetics and pharmacodynamic in early stages of drug discovery. In the present study, we aimed at identifying the most reliable and practical in vitro approach to establish good IVIVC in rat. Twelve OATP substrates with diverse physicochemical properties were selected for this investigation. For most of the compounds, OATP1B1 is the dominant uptake transporter responsible for the hepatic uptake, except telmisartan, which is only transported by OATP1B3 (Supplemental Table 1). The hepatic uptake has been proven to be the rate-determining step for hepatic CL for these compounds, as indicated by preclinical and clinical evidence (Supplemental Table 1). In addition, uptake in rat hepatocyte in the absence and presence of 4% BSA was conducted to investigate the impact of albumin on intrinsic hepatic uptake CL ($PS_{u,inf}$) and Kp_{uu} estimation. Subsequently, these in vitro parameters were used to predict hepatic CL via two advanced IVIVE approaches: 1) directly predicting the hepatic CL using the initial uptake CL determined in rat hepatocytes suspension in the absence or presence of 4% BSA and 2) prediction based on intrinsic metabolic CL with correction of the Kp_{uu} according to the extended clearance concept.

Materials and Methods

Chemicals and Reagents

Rosuvastatin calcium, atorvastatin calcium, pravastatin sodium, pitavastatin calcium, glyburide, valsartan, and telmisartan were purchased from MilliporeSigma (St. Louis, MO). Fluvastatin sodium and cerivastatin were purchased from Tocris bioscience (Bristol, UK). Bosentan was purchased from Bosche Scientific (New Brunswich, NJ). Asunaprevir was obtained from Advanced ChemBlock Inc (Burlingame, CA), and nateglinide was obtained from Tokyo Chemical Industry Co, Ltd. (Tokyo, Japan). Rifamycin SV sodium salt was purchase from MP Biomedicals, LLC (Solon, OH). Cryopreserved rat hepatocytes (lot JTJ), Krebs-Henseleit buffer (KHB), pooled rat plasma, and rat liver homogenates were purchased from Bioreclamation IVT, LLC (Hicksville, NY). The cryopreserved hepatocyte thawing medium (CHRM) was obtained from APSciences, Inc. (Columbia, MD). Dulbecco's modified Eagle's medium (DMEM) and L-glutamine were obtained from Thermo Fisher Scientific (Waltham, MA). Dimethyl sulfoxide and bovine serum albumin were purchased from MilliporeSigma. HPLC grade acetonitrile and water were purchased from Burdick & Jackson (Muskegon, MI).

Permeability Determination

Transcellular permeability studies using Madin-Darby Canine Kidney (MDCKII) epithelial cell monolayers were conducted at Q^2 Solutions (Indianapolis, IN). Briefly, transcellular assay was performed on day 4 after plating of the MDCKII cells on 96-well transwell plates. Cells were preincubated with assay buffer (Hanks' balanced salt solution, pH 7.4, supplemented with 10 mM Hepes, 1 μM elacridar, and 0.1% BSA) for 30 minutes. After preincubation, assay buffer containing 5 μM test compound was added into the apical compartment, and assay buffer alone was added to the basal compartment. Elacridar (1 μM) was added to assay buffer at all times to inhibit any endogenous P-glycoprotein activity. Each incubation was performed in triplicate. The plates were reassembled and incubated (37°C, 5% CO_2) for 2 hours. At the end of incubation, samples from receiver and donor compartments were collected and analyzed by liquid chromatography–tandem mass spectrometry (LC-MS/MS), and the apparent permeability coefficient (P_{app}) of tested compounds was calculated: $P_{AB} = (dQ/dt)/(A * C_0)$, where dQ/dt is the apical-to-basal penetration rate of the agent, A is the surface area of the cell monolayer on the transwell, and C_0 is the initial concentration of the test compound.

Determination of Unbound Fraction in Different Biologic Matrices

The binding in rat plasma, rat liver tissue homogenate, and KHB buffer containing 4% BSA and hepatocyte suspension was performed using ultracentrifugation method as previously described with slight modification (Nakai et al., 2004). Rat liver homogenate was prepared as 1 g tissue per 4 ml of phosphate-buffered saline (dilution factor = 5). Briefly, rat plasma, diluted liver tissue homogenate, and KHB with 4% BSA were spiked with test article at concentration of 5 μM and hepatocyte suspension at concentration 0.5 μM. Thereafter, 25 μl aliquots of spiked matrix were transferred to a sample plate and kept on ice to represent total drug. Aliquots (220 μl) were transferred to ultracentrifuge tubes and spun at 190,000*g* for 4.5 hours in a Type 42.2 rotor (Beckman Coulter) at 37°C. The remainder of spiked plasma was incubated at 37°C for the duration of the centrifugation period to be used to evaluate stability of test article. After centrifugation, 25 μl aliquots of the aqueous supernatant representing unbound fractions and the stability control plasma were transferred to the sample plate. Samples were matrix matched and quenched with cold acetonitrile with 0.1% formic acid containing internal standard (1 μM tolbutamide). The samples were vortex-mixed and centrifuged at 3400*g* for 15 minutes at 4°C. The supernatants were analyzed by liquid chromatography-mass spectrometry using a Waters Acquity H-Class ultraperformance liquid chromatography system with a BEH C18 column (1.7 μm × 2.1 × 50 mm) connected to a Q Exactive Hybrid Quadrupole-Orbitrap Mass Spectrometer (Thermo Scientific) in full scan positive mode. The unbound fraction in rat plasma ($f_{u,\ plasma}$) and KHB with 4% BSA ($f_{u,\ BSA}$) was calculated from the ratio of analyte detected in the aqueous layer after centrifugation relative to the total concentration in the original matrix. The fraction unbound in tissue homogenates was corrected for dilution according to the equation described in Kalvass et al. (2007):

$$\text{Undiluted } f_u = \left(\frac{1/D}{\left(\left({}^1/_{f_u} \right) - 1 \right) + 1/\text{D}} \right) \quad (1)$$

where undiluted f_u is the adjusted fraction unbound in tissue, f_u is the measured fraction unbound assuming no dilution, and D is the fold dilution of the tissue.

Measurement of $CL_{int,met}$ by Using Cryopreserved Rat Hepatocytes

Intrinsic metabolic CL was determined using cryopreserved Sprague-Dawley rat hepatocytes in suspension (Lot JTJ) in the standard 1-hour incubation assay. Cryopreserved rat hepatocytes were thawed and recovered in prewarmed CHRM. After a quick centrifugation at 100*g* for 10 minutes, the cells were reconstituted in prewarmed DMEM (Thermo Fisher Scientific) supplemented with 2 mM L-glutamine (Thermo Fisher Scientific). The hepatocytes with equal or greater than 80% viability were diluted to 0.5×10^6 cells/ml in prewarmed DMEM. The reaction was initiated by spiking test compounds into the hepatocyte suspension to achieve a final concentration of 0.5 μM and incubated at 37°C in a humidified CO_2 incubator for 1 hours on a thermomixer shaker. At 0, 10, 20, 30, 45, and 60 time points, the reaction was stopped by adding quench solution (acetonitrile with 0.1% formic acid with tolbutamide as internal standard). After centrifugation at 3750*g* for 45 minutes, the supernatants were analyzed for test compound and internal standard by RapidFire 365 high-throughput solid-phase extraction system interfaced with a 6550 quadrupole time-of-flight mass spectrometer (Agilent) (Supplemental Methods). The apparent metabolic intrinsic clearance $CL_{int,\ met}$ (microliters per minute per 10^6 cells) was determined based on the degradation half-life estimated from analyte to internal standard peak area ratio time profile data.

In Vitro Uptake Assay in Rat Hepatocytes Suspension

Uptake assay was performed in cryopreserved rat hepatocytes in suspension using a centrifugal filtration method described previously (Hirano et al., 2004). Cryopreserved rat hepatocytes (Lot JTJ) were thawed and recovered in prewarmed CHRM. After a quick centrifugation at 100*g* for 10 minutes, the cells were reconstituted in ice-cold KHB in the absence or presence of 8% bovine serum albumin at cell density of 1.0×10^6 cells/ml. Hepatocytes with greater than 85% viability were used in all the uptake study described below. The cells (2× final concentration) were aliquoted into glass tube and stored on ice before use. The hepatic uptake was evaluated for the initial uptake rate by collecting aliquots at short time intervals (e.g., 20, 45, and 90 seconds or 30, 60, and 120 seconds) up to 30 minutes at 37°C in the presence or absence of 1 mM rifamycin SV. The passive diffusion was also assessed on ice with assumption that all the active uptake is abolished at 4°C. After 5-minute preincubation at 37°C or on ice, the uptake was initiated by adding an equal volume of prewarmed or prechilled KHB containing 2× test compound, resulting in the final test compound concentration of 1 μM and cell concentration of 0.5×10^6 cells/ml. At the designated time, an 80-μl aliquot of the reaction was removed and loaded onto a 0.4 ml centrifugation tube (Thermo Fisher Scientific) containing 100 μl of silicone–mineral oil layer (5:1 ratio, density of 1.015 g/ml) over 50 μl of 2 M ammonium acetate to separate the hepatocytes from the reaction buffer. The top layer medium samples and hepatocyte pellets were vortex-mixed with quenching solution (80% acetonitrile with 0.1% formic acid containing internal standard, 100 nM tolbutamide). After centrifugation at 4000 rpm for 20 minutes, the supernatants were analyzed by LC-MS/MS using API 5500 triple quadrupole mass spectrometer with Turbo Ion Spray source in multiple reaction monitoring mode (AB Sciex, Foster City, CA) (Supplemental Methods).

Rat PK Study

The intravenous PK studies in rats were conducted at Syngene International Limited (Bangalore, India). Male Sprague-Dawley rats, 8–10 weeks old, weighing between 250 and 350 g, were dosed either rosuvastatin, fluvastatin, cerivastatin, or pravastatin (each prepared in 100% DMSO) at 1 mg per kg single dose, via intravenous bolus injected in femoral vein. The dosing volume was controlled at 0.5 ml/kg. Serial blood sampling was done via jugular vein at 0.083, 0.25, 0.5, 1, 2, 4, 6, 8, and 24 hours after dose. Blood samples collected in K2-EDTA tubes were placed on ice until centrifuged (at 4°C, 10 minutes at 13,000 rpm, within 30 minutes of collection) to separate plasma. Plasma samples were stored at −70°C until LC-MS/MS analysis.

Data Analysis

Approach 1: Determination of Initial Hepatic Uptake CL ($PS_{u,inf}$) from In Vitro Hepatocyte Uptake Assay. The initial uptake rate was estimated from the slope obtained from the time course data within the initial linear phase, usually the first three time points (20, 45, and 90 seconds or 30, 60, and 120 seconds) using linear regression analysis. In the absence of BSA, the uptake CL (PS_{inf}) was calculated by dividing the initial uptake velocity by the total drug concentration measured in the incubation buffer. Assuming minimal binding in the aqueous buffer, PS_{inf} is equal to $PS_{u,\ inf}$. In the presence of BSA, the uptake CL ($PS_{u,\ inf}$) was determined by dividing the initial uptake velocity by the unbound drug concentrations in the incubation buffer containing 4% BSA.

$$PS_{u,inf} = \frac{PS_{inf}}{f_{u,\ KHB\ w\ 4\%\ BSA}} \quad PS_{u,\ inf} = PS_{u,\ act} + PS_{u,dif}$$

Approach 2: Determination of Kp_{uu} in Rat Hepatocytes.

Determination of $Kp_{uu,ss}$ in rat hepatocytes based on steady-state uptake. The time-dependent uptake profiles for the transporter substrates were limited to 30 minutes to ensure good viability of hepatocytes. For most of the compounds, the uptake peaked or reached plateau at 5 or 15 minutes. Based on the assumptions that the active uptake and efflux in hepatocytes are completely ceased on ice and the fraction unbound in the cell at steady state is independent of temperature, the Kp_{uu} can be determined as Kp ratio of 37°C versus 4°C at steady state ($Kp_{uu,ss}$).

In the absence of BSA, at steady state, it is assumed to reach equilibrium between intracellular compartment and medium, so $C_{u,\ cell}$ (4°C) = $C_{u,media}$ (4°C) and $f_{u,cell}$ (4°C) = $f_{u,cell}$ (37°C).

In the absence of BSA, it is assumed that $f_{u,media} = 1$

$$f_{u,cell,\ 4oC} = \frac{C_{u,\ cell\ (4^oC)}}{C_{cell\ (4^oC)}} = \frac{C_{u,\ media\ (4^oC)}}{C_{cell\ (4^oC)}} = \frac{1}{Kp_{4^oC}}$$

$$Kp_{uu,ss} = \frac{C_{u,\ cell\ 37^oC}}{C_{u,media\ 37^oC}} = \frac{C_{cell\ 37^oC} \times f_{u,cell}}{C_{media\ 37^oC} \times f_{u,media}} = \frac{Kp_{37^oC}}{Kp_{4^oC}}$$

In the presence of BSA, $f_{u,media}$ is $f_{u,KHB\ w\ 4\%\ BSA}$

$$f_{u,cell,\ (4^oC)} = \frac{C_{u,\ cell\ (4^oC)}}{C_{cell\ (4^oC)}} = \frac{C_{u,\ media\ (4^oC)}}{C_{cell\ (4^oC)}} = \frac{C_{media\ (4^oC)} \times f_{u,\ KHB\ w\ 4\%BSA}}{C_{cell\ (4^oC)}} = \frac{f_{u,\ KHB\ w\ 4\%BSA}}{Kp_{4^oC}}$$

$$Kp_{uu,ss} = \frac{C_{u,\ cell\ 37^oC}}{C_{u,media\ 37^oC}} = \frac{C_{cell\ 37^oC} \times f_{u,cell}}{C_{media\ 37^oC} \times f_{u,KHB\ w\ 4\%BSA}} = \frac{Kp_{37^oC}}{Kp_{4^oC}}$$

where the Kp was determined by the ratio of total hepatocyte concentration and medium concentration at 15 minutes.

When the hepatic uptake reaches steady state in vitro, the unbound hepatocyte-to-medium concentration ratio (Kp_{uu}) can be also determined by the equation below:

$$Kp_{uu,ss} = \frac{C_{u,\ cell,ss}}{C_{u,media,ss}} = \frac{C_{cell,ss} \times f_{u,cell}}{C_{media,ss} \times f_{u,media}} = Kp \times \frac{f_{u,cell}}{f_{u,media}}$$

In the absence of BSA, it is assumed that $f_{u,media} = 1$

$$Kp_{uu,ss} = Kp \times f_{u,cell}$$

In the presence of BSA,

$$Kp_{uu,ss} = Kp \times \frac{f_{u,cell}}{f_{u,\ KHB\ w\ 4\%\ BSA}}$$

where the $f_{u,cell}$ and $f_{u,KHB\ w\ 4\%\ BSA}$ were experimentally determined in the binding assay.

Determination of $K_{puu,V0}$ in rat hepatocytes based on initial uptake rate. CL_{uptake} consists of active uptake ($PS_{inf,act}$) and passive diffusion ($PS_{inf,dif}$). PS_{inf} was determined by the initial hepatic uptake CL determined at 37°C, whereas the PS_{dif} was determined by the initial hepatic uptake CL determined at 37°C in the presence of uptake inhibitor, rifamycin SV. Based on the extended clearance concept, assuming that the PS_{dif} for the cellular influx is equal to that for the efflux, $K_{p,uu}$ based on the initial uptake rate can be calculated using

$$Kp_{uu,V0} = \frac{PS_{inf}}{PS_{dif}} = \frac{PS_{act} + PS_{dif}}{PS_{dif}}$$

IVIVE for Hepatic CL. The intrinsic hepatocyte metabolic CL ($CL_{int,\ met}$ microliters per minute per 10^6 cells) was determined in the absence of BSA in rat

hepatocytes, and the in vitro unbound hepatic uptake CL ($PS_{u,inf}$, microliters per minute per 10^6 cells) was first scaled up to in vivo using the following physiologic scaling factor: 108 million cells/g liver and 36 g liver/kg body weight (SimCYP).

According to the extended clearance concept (Sirianni and Pang 1997; Shitara et al., 2006; Kusuhara and Sugiyama 2009; Patilea-Vrana and Unadkat 2016), the hepatic intrinsic clearance ($CL_{int,\ all}$) is described by the following equation:

$$Cl_{int,\ all} = (PS_{inf,act} + PS_{inf,\ dif}) \times \frac{CL_{int,met+bile}}{PS_{eff,act} + PS_{eff,\ dif} + CL_{int,met+bile}}$$

where $PS_{inf,act}$, $PS_{inf,dif}$, $PS_{eff,act}$, $PS_{eff,dif}$ and $CL_{int,\ met+bile}$ represents transporter-mediated active uptake intrinsic CL, intrinsic passive diffusion influx CL, intrinsic transporter-mediated active efflux CL, intrinsic passive diffusion sinusoidal efflux CL, and the sum of intrinsic metabolic clearance ($CL_{int,\ met}$) and biliary excretion ($CL_{int,\ bile}$).

If $CL_{int,\ met+bile}$ is much higher than the total back flux ($PS_{eff,\ dif}$, and $PS_{eff,act}$), then $CL_{int,\ all}$ can be described as the following:

$$Cl_{int,all} = PS_{inf,act} + PS_{inf,\ dif}$$

The equation can be rewritten as the following:

$$Cl_{int,\ all} = (CL_{int,met+bile}) \times \frac{PS_{inf,act} + PS_{inf,\ dif}}{PS_{eff,act} + PS_{eff,\ dif} + CL_{int,met+bile}}$$

where $(PS_{inf,act} + PS_{inf,dif})/(PS_{eff,act} + PS_{eff,dif} + CL_{int,\ met+bile})$ represents to the degree of hepatocellular unbound drug accumulation or the liver to plasma drug unbound concentration ratio (Kp_{uu}) at steady state. For the compounds that are actively taken up by hepatic uptake transporters and eliminated primarily by enzymatic metabolism, the equation is described as follows:

$$CL_{int,all} = CL_{int,met} \times Kp_{uu}$$

The predicted overall hepatic intrinsic clearance, by the above described methods, was used to predict systemic plasma clearance (CL_H) mediated by hepatic elimination using well stirred model (Pang and Rowland, 1977),

$$CL_H = Q_H \times \frac{CL_{int} \times f_{u,p}}{CL_{int} \times \frac{f_u}{R_{B/P}} + Q_H}$$

where CL_{int}, Q_H, $f_{u,p}$, and $R_{B/P}$ represent the predicted intrinsic hepatic CL, rat hepatic blood blow (77 ml/min per kilogram), and unbound fraction in rat plasma and blood to plasma ratio, respectively.

The hepatic CL predicted by each IVIVE method was compared with the observed systemic CL. As the renal CLs in rat for all the selected compounds are minimal (<10%), the total plasma clearance (CL_P) was used as surrogate of hepatic CL.

Statistical Analysis

The prediction performance of each IVIVE approach used in the study was compared with observed hepatic CL in rat. The fold error, absolute average fold error (AAFE), and root mean squared logarithmic error (RMSLE) were calculated by the following equations:

$$fold\ error = 10^{\left|Log_{10}\left(\frac{CL_{pred}}{CL_{observed}}\right)\right|}$$

$$AAFE = 10^{\left[\frac{1}{n}\sum\left|Log\left(\frac{CL_{pred}}{CL_{observed}}\right)\right|\right]}$$

$$RMSLE = \sqrt{\frac{1}{n}\sum(Log\ (CL_{pred}+1) - Log(CL_{observed}+1))^2}$$

Results

Physicochemical Properties and In Vitro ADME Data of Selected OATP Substrates. Twelve structurally diverse organic anion drugs covering a broad spectrum of physicochemical properties were systematically selected on the basis of varying permeability and lipophilicity. Compounds with high lipophilicity and high permeability include fluvastatin, cerivastatin, atorvastatin, bosentan, telmisartan, pitavastatin, nateglinide, and glyburide; compounds with lower lipophilicity and low permeability include rosuvastatin, pravastatin, and valsartan; a compound with high lipophilicity and low permeability includes asunaprevir. The permeability and unbound fraction in all the matrices, including rat liver homogenate, KHB containing 4% BSA, rat plasma and rat hepatocyte incubation, and $CL_{int,\ met}$ in rat hepatocytes were determined and summarized in Table 1 along with the physicochemical properties for each compound. The overall Log D at pH 7.4 spans from −2.7 to 4.0, and the permeability spans from 0.14 to 29 (10^{-6} cm/s). The unbound fractions in KHB with 4% BSA ($f_{u,\ KHB\ w\ 4\%\ BSA}$) were within 2–3-fold of the unbound fractions in rat plasma ($f_{u,p}$) for pravastatin, valsartan, fluvastatin, cerivastatin, and atorvastatin. For the rest of compounds, the difference of $f_{u,\ KHB\ w\ 4\%\ BSA}$ value with $f_{u,p}$ value was greater than 3-fold. The $f_{u,p}$ values for almost all drugs except rosuvastatin and pravastatin were less than 0.05; and $f_{u,p}$ values for valsartan, pitavastatin, bosentan, glyburide, and telmisartan were less than 0.01. For the drugs with highest lipophilicity, i.e., telmisartan and asunaprevir, the unbound fraction in rat liver homogenate was less than 0.01, suggesting high nonspecific binding for these two compounds.

Effect of Albumin on Hepatic Uptake CL in Rat Hepatocyte Suspension. The time-dependent uptake profile was determined in rat hepatocyte suspension in the absence and presence of 4% BSA (Fig. 1). The uptake velocity at 4°C of all the test compounds was significantly lower than that at 37°C. In the presence of hepatic uptake transporter inhibitor, rifamycin SV, the uptake at 37°C significantly decreased for all of the compounds confirming the involvement of active uptake transport. However, only for the less permeable compounds, i.e., rosuvastatin, pravastatin and valsartan, the uptake at 37°C with inhibitor was reduced to the levels similar to 4°C. With addition of BSA, the dynamic range of active uptake (uptake at 37° C vs. uptake at 37°C with inhibitor) improved, particularly for the two highly lipophilic drugs with high nonspecific binding, asunaprevir (from less than 2-fold to 4-fold) and telmisartan (from 3-fold to 6-fold). In the absence of BSA, the uptake of all the drugs increased in a time-dependent manner except for telmisartan. The uptake of telmisartan reached a steady state instantaneously due to its high binding characteristic, resulting in instant binding onto the cell surface. Therefore, the PS_{inf} at 37°C of telmisartan was not determined in the pure aqueous buffer system. In the presence of BSA, the uptake of all the drugs increased in a time-dependent manner. Initial hepatic uptake CL (PS_{inf}) was determined from the initial slopes of uptake measured in KHB and KHB containing 4% BSA, respectively (Table 2). In the presence of BSA, the hepatic uptake CL for unbound drug ($PS_{u,inf}$) was calculated by dividing PS_{inf} by $f_{u,\ KHB\ w\ 4\%BSA}$ value. In the regular KHB, unbound fraction in the medium was assumed to be unity; therefore, the $PS_{u,inf}$ was equal to PS_{inf}. In the absence of BSA, $PS_{u,inf}$ ranged from 8.9 (pravastatin) to 2210 (asunaprevir) μl/min per 10^6 cells, and in the presence of BSA, $PS_{u,inf}$ ranged from 10.3 (pravastatin) to 2668 (asunaprevir) μl/min per 10^6 cells. In the presence of BSA, the PS_{inf} values for almost all drugs except pravastatin decreased compared with PS_{inf} values determined in the absence of BSA. However, the $PS_{u,inf}$ with BSA overall increased, but to different extents, when compared with $PS_{u,inf}$ without BSA: for rosuvastatin, cerivastatin, pravastatin, atorvastatin, bosentan, asunaprevir, and nateglinide, this increase was less than 2-fold; for fluvastatin, pitavastatin, and glyburide, the increase was within 2–3-fold; for valsartan and telmisartan, the increase was greater than 10-fold. These results demonstrated that drugs with high plasma protein binding vary in the level of "albumin-mediated" hepatic uptake. Additionally, based on these data we were unable to identify any specific trends related to permeability or lipophilicity of the compounds that would dictate the enhanced hepatic uptake in the presence of BSA.

TABLE 1

Physicochemical properties, unbound fraction in variety of matrices, intrinsic metabolic clearance in rat hepatocytes of the selected 12 compounds

	Physicochemical properties				Unbound fraction in matrices				Intrinsic metabolic CL
	M.W.	Log $D_{7.4}$[a]	pKa[a]	P_{app} 10^{-6} cm/s	$f_{u,\ liver\ tissue}$	$f_{u,\ KHB\ w\ 4\%BSA}$	$f_{u,\ p}$	$f_{u,\ hep}$	Rat hepatocyte $CL_{int,met}$ µl/min per 10^6 cells
Rosuvastatin	481.5	−2.7	4.3	1.8	0.15	0.21	0.059	0.77	19.8
Pravastatin	424.5	−0.8	4.3	0.62	0.29	0.69	0.63	0.85	NA
Valsartan	435.5	−0.6	3.7, 4.2	0.14	0.048[b]	0.006[c]	0.0029	0.79	20.4
Pitavastatin	421.5	0.4	4.2, 5.2	13	0.019	0.057	0.0065	0.56	46.2
Fluvastatin	411.5	0.5	4.3	19	0.015	0.037	0.015	0.51	38.8
Cerivastatin	459.6	0.6	4.2, 5.6	28	0.019	0.04	0.029	0.59	47.9
Nateglinide	317.4	0.6	3.6	6.2	0.037	0.063	0.015	0.73	43.5
Atorvastatin	558.6	1.3	4.3	5.5	0.018	0.066	0.036	0.63	90.8
Bosentan	551.6	1.5	4.0	16	0.025	0.057	0.0089	0.66	39.4
Glyburide	494.0	1.9	5.2	22	0.011	0.014	0.002	0.60	54.5
Asunaprevir	748.3	2.3	3.9, 5.6	1.7	0.00073	0.059	0.013	0.31	36.2
Telmisartan	514.6	4.0	3.5, 3.9, 5.0	29	0.0038	0.031	0.0061	0.45	23.3

NA, not available. M.W.; Molecular Weight
[a]Predicted by Amgen in silico model.
[b]Data are referenced from Li et al. (2014).
[c]Data are referenced from Riccardi et al. (2019).

Effect of Albumin on Kp_{uu} Determination in Rat Hepatocytes. The Kp_{uu} values of the 12 OATP substrates were determined in the absence and presence of BSA using temperature method, homogenization method and initial rate method as described in the *Materials and Methods* section. The data are summarized in Table 3. Based on the time profiles, the uptake of most drugs peaked at 15 minutes, then either plateaued or started to decline. For both temperature method and homogenization method, the $Kp_{uu,\ ss}$ were determined at 15 minutes for all the compounds, except valsartan determined at 30 minutes of uptake. By using the temperature method, the difference of $Kp_{uu,ss}$ values determined in the absence or presence of BSA were mostly within 2–3-fold. In contrast, using homogenization method in general resulted in an increase in the $Kp_{uu,ss}$ values, except for rosuvastatin, pravastatin and bosentan. The increase was substantial (greater than 7-fold) for valsartan, telmisartan and glyburide; for the rest of compounds, the increase was within 2-fold. PS_{inf} and $PS_{inf,dif}$ were determined from the initial slope of uptake at 37°C without and with inhibitor, respectively. The $Kp_{uu,V0}$ calculated based on ratio of PS_{inf} and $PS_{inf,dif}$ determined in the absence and presence of BSA are summarized in Table 3. The impact of BSA on the $Kp_{uu,V0}$ does not have a clear trend due to the relatively large interexperimental variability. $Kp_{uu,V0}$ for telmisartan in the absence of BSA cannot be determined due to the high nonspecific binding.

In Vitro to In Vivo Extrapolation of Hepatic CL. The hepatic CL predicted by three IVIVE approaches using 1) $CL_{int,\ met}$ alone, 2) $CL_{int,\ met}$ corrected by Kp_{uu}, and 3) $PS_{u,inf}$ were compared with in vivo observed hepatic CL in rat (Fig. 2). First, when applying the traditional IVIVE approach by scaling directly from intrinsic metabolic CL alone, the hepatic CL was significantly underestimated for majority of the compounds, and the AAFE and RMSLE were 8.99 and 0.83, respectively (Table 5). Only one compound (atorvastatin) fell within 3-fold error, and 6 out of 12 compounds showed greater than 10-fold underestimation of the hepatic CL (Fig. 2A; Table 4).

Based on the extended clearance concept, in the scenario when hepatic uptake is the rate-determining step for hepatic CL, the intrinsic hepatic CL could be well accounted for by the in vitro hepatic uptake CL, regardless of the involvement of hepatic metabolism. $PS_{u,inf}$ determined in the hepatic uptake assay was used to predict the systemic hepatic CL (Fig. 2B; Table 2). In the absence of BSA, 5 out of 12 compounds fell within the 3-fold error; 9 out of 12 compounds fell within 5-fold error; two compounds (valsartan and nateglinide) showed great than 10-fold underestimation; this approach was not applicable for telmisartan as $PS_{u,inf}$ could not be determined. In the presence of BSA, the predictability of $PS_{u,inf}$ was improved as demonstrated by AAFE and RMSLE (3.48 and 0.58 without BSA vs. 2.23 and 0.40 with BSA) (Table 5); 8 out of 12 compounds fell within the 3-fold error and 11 out of 12 compounds fell within 5-fold error; only one compound (nateglinide) was underestimated greater than 5-fold.

According to the extended clearance concept, correcting $CL_{int,\ met}$ determined in rat hepatocytes by multiplying Kp_{uu} substantially improved the prediction of hepatic CL for all of the 12 compounds (Table 4). When using the $Kp_{uu,ss}$ determined by temperature method in the absence of BSA, the prediction of 10 out 12 compounds fell within the 3-fold error, and only one compound (telmisartan) showed greater than 5-fold underestimation of the hepatic CL (Fig. 2C). In the presence of BSA, the prediction performance was similar with the condition without BSA, as demonstrated by AAFE and RMSLE (1.95 and 0.32 without BSA vs. 2.11 and 0.37 with BSA) (Table 5). When using the $Kp_{uu,ss}$ determined by homogenization method, in the absence of BSA, 6 out of 12 compounds fell within the 3-fold error, and four compounds (valsartan, telmisartan, asunaprevir, and nateglinide) showed greater than 5–10-fold underestimation (Fig. 2D). In contrast, the prediction performance was significantly improved by applying BSA when using the homogenization method, as demonstrated by AAFE and RMSLE (3.72 and 0.58 without BSA vs. 2.0 and 0.35 with BSA) (Table 5). When using the $Kp_{uu,v0}$ determined by the ratio of PS_{inf} and $PS_{inf,dif}$, 9 out of 12 compounds fell within the 3-fold error regardless of the presence of BSA (Fig. 2E). Although the prediction performance of the $Kp_{uu,v0}$ approach looked reasonable, due to the large interexperimental variation of $Kp_{uu,v0}$ determination, this method is not practically recommended.

Discussion

Accurate human PK prediction is pivotal at early stages of drug discovery to manage human dose projection and to estimate efficacy and safety margins in an integrated manner. With the success in reducing cytochrome P450–mediated CL, the current chemical matter of interest has become more metabolically stable, and transporter-mediated CL mechanisms have become predominant drivers of clearance (Shitara et al., 2006, Giacomini et al., 2010; Jones et al., 2012). A practical

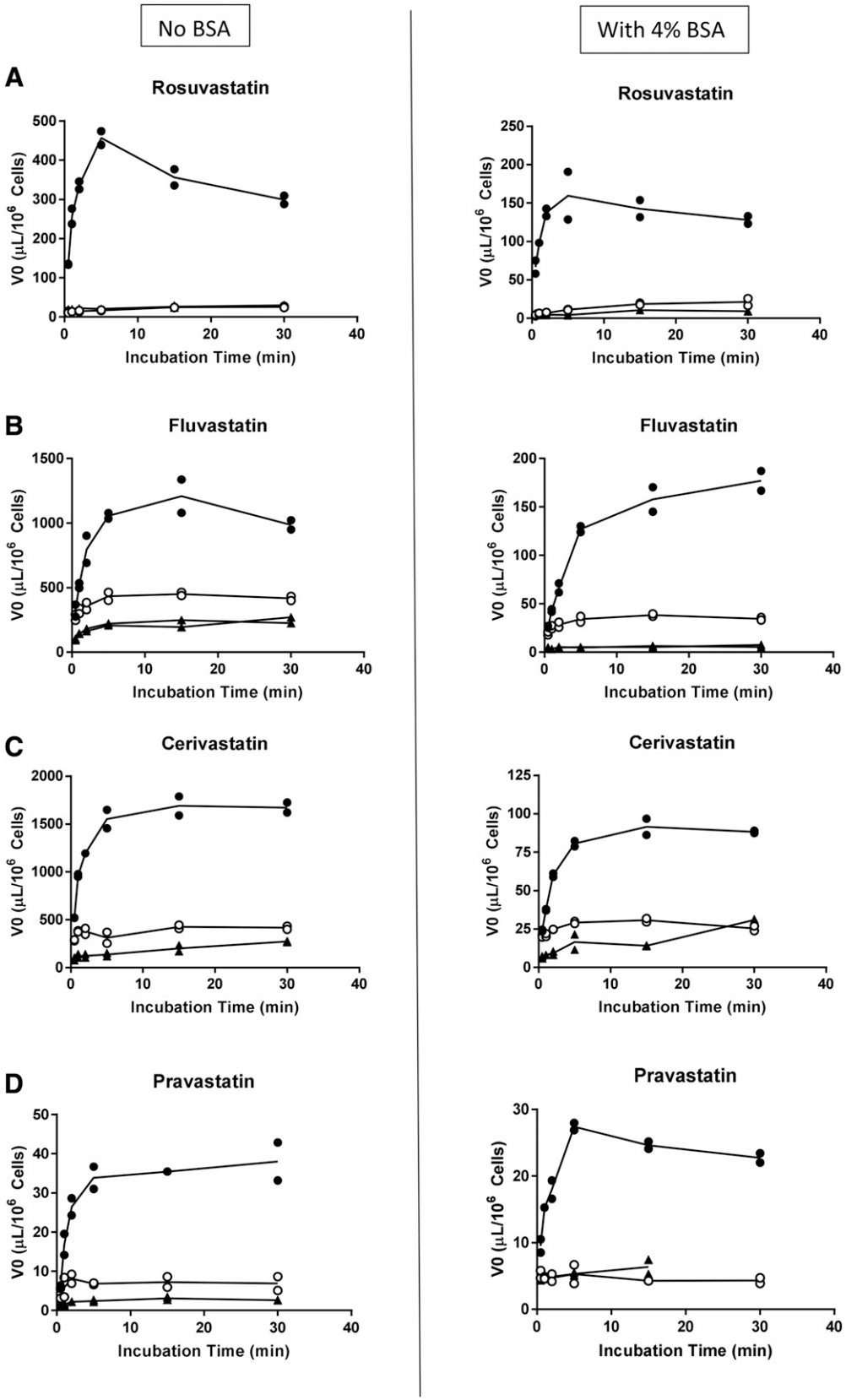

Fig. 1. Time-dependent uptake of the 12 OATP substrates in cryopreserved rat hepatocyte suspension. Uptake of rosuvastatin (A), fluvastatin (B), cerivastatin (C), pravastatin (D), atorvastatin (E), pitavastatin (F), bosentan (G), glyburide (H), nateglinide (I), valsartan (J), asunaprevir (K), and telmisartan (L) at 1 μM was determined in the regular KHB (left column) or KHB containing 4% BSA (right column) for (20 seconds to 30 minutes) at 37°C (closed circle), 37°C in the presence of 1 mM rifamycin SV (open circle), or 4°C (closed triangle). The uptake velocity (V_0) was calculated by dividing the amount of compound measured in rat hepatocytes at each time point by the total compound concentration in the reaction buffer in the absence or presence of 4% BSA. Data represent duplicate measurement at each time points.

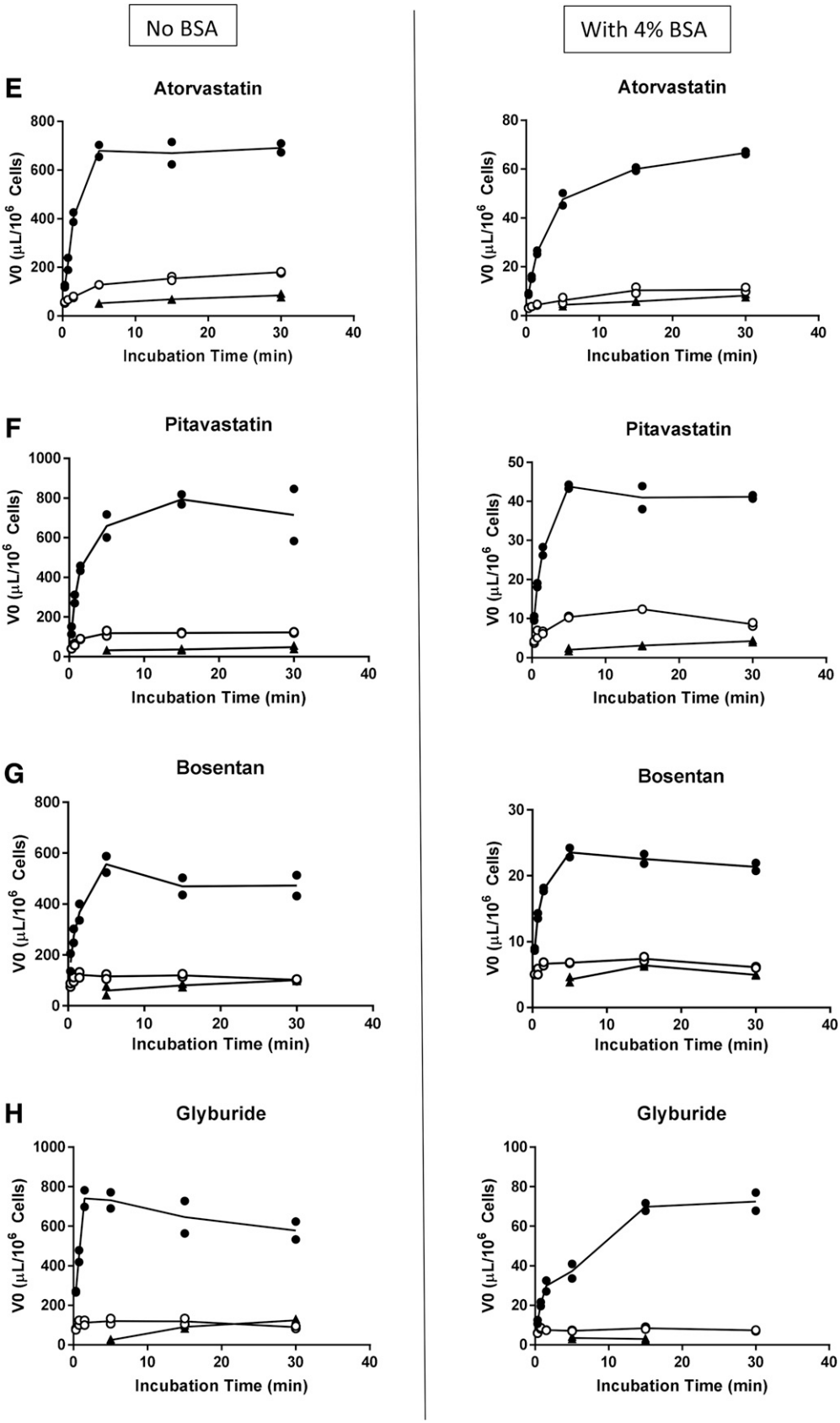

Fig. 1. Continued.

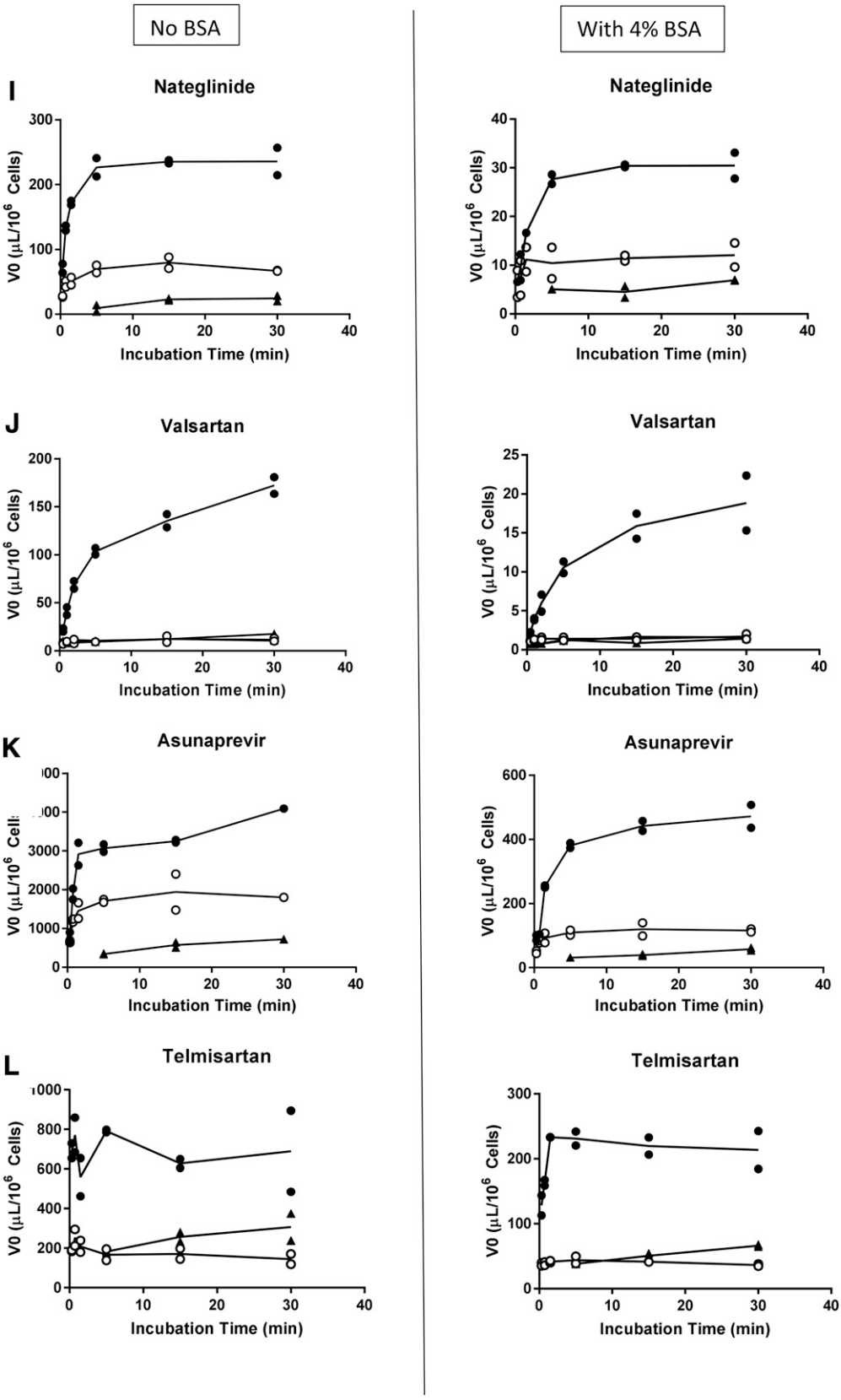

Fig. 1. Continued.

TABLE 2

Unbound initial hepatic uptake clearance determined in the presence and absence of 4% BSA and predicted rat hepatic clearance

The $PS_{u,inf}$ data are presented as either means of two independent experiments (individual data are given in parentheses) or means ± S.D. of three to five independent experiments.

Compound	Initial hepatic uptake rate		Predicted hepatic CL				Observed CL
	no BSA	with 4% BSA	no BSA		with 4% BSA		
	$PS_{u,\ inf}$ μl/min per 10^6	$PS_{u,\ inf}$ μl/min per 10^6	CL_{int} ml/min per kilogram	Pred rat CL ml/min per kilogram	CL_{int} ml/min per kilogram	Pred rat CL ml/min per kilogram	Rat CL ml/min per kilogram
Rosuvastatin	120 (126, 114)	221 ± 13.8	467	17.2	858	24.2	56.7
Pravastatin	8.87 (13.0, 4.73)	10.3 (7.49, 13.2)	34.5	14.8	40.2	16.4	59.7
Valsartan	34.0 ± 10.5	560 (404, 716)	132	0.4	2177	5.6	17.8[a]
Pitavastatin	249 (261, 236)	470 ± 212	966	5.5	1827	9.4	28[b]
Fluvastatin	277 (310, 244)	903 (710, 1095)	1077	12.0	3509	24.6	20.0
Cerivastatin	527 ± 110	798 (595, 1001)	2048	26.0	3103	30.5	24.7
Nateglinide	88.8 (82.4, 95.1)	144 (139, 149)	345	4.7	560	7.1	58.1[c]
Atorvastatin	300 (244, 355)	311 ± 110	1164	22.0	1210	22.4	35[b]
Bosentan	232 (166, 297)	231 ± 94	900	6.8	899	6.8	23[d]
Glyburide	461 (403, 518)	1587 (1078, 2095)	1790	3.3	6168	9.7	6.8[e]
Asunaprevir	2210 (1759, 2661)	2668 (2454, 2882)	8592	32.7	10,373	34.4	38.4[f]
Telmisartan	ND (n = 2)	2625 ± 462	ND	ND	10,205	26.5	14.6[g]

ND, not detected.
[a]Data are referenced from Yamashiro et al. (2006).
[b]Data are referenced from Watanabe et al. (2010).
[c]Data are referenced from Tamura et al. (2010).
[d]Data are referenced from Treiber et al. (2004).
[e]Data are referenced from Zhou et al. (2016).
[f]Data are referenced from Mosure et al. (2015).
[g]Data are referenced from Wienen et al. (2000).

approach to accurately predict transporter-mediated CL is urgently needed in the field to guide the prioritization of the new molecular entities with suitable PK properties for clinical development. Gaining the confidence in IVIVE strategies in preclinical species is an essential step toward improved human PK prediction. Rat is the most commonly used preclinical species for evaluating PK of drug candidates in early drug discovery. Therefore, this study focused on establishing a robust in vitro uptake assay using rat hepatocytes and evaluating a variety of IVIVE approaches to provide a practical solution for predicting hepatic uptake transporter-mediated clearance in rat.

It has also been demonstrated that the intrinsic hepatic uptake CL determined in human hepatocytes suspension was far more predictive of in vivo clearance of statins than extrapolating from intrinsic metabolic clearance (Watanabe et al., 2010, 2011). However, this approach is restricted to highly lipophilic compounds, due to the inability to detect active transport activity due to the high background caused by the high permeability, and underestimation of the intrinsic hepatic uptake clearance due to the nonspecific binding (Kim et al., 2019; Koyanagi et al., 2019). Several studies have reported that addition of albumin can improve the IVIVE for hepatic uptake transporter substrates (Kim et al., 2019; Koyanagi et al., 2019; Riccardi et al., 2019). Therefore, in the current study, we investigated the impact of BSA at physiologically relevant concentrations on the predictability of the hepatic uptake parameters determined in suspended rat hepatocytes using various approaches.

Compared with the traditional IVIVE approach from $CL_{int,\ met}$ alone, both advanced approaches ($PS_{u,inf}$ and $CL_{int,\ met}$ corrected by Kp_{uu}) substantially improved the prediction of hepatic CL for all 12 selected drugs. Among all the conditions evaluated in this study, $PS_{u,inf}$ generated in the presence of 4% BSA and $CL_{int,\ met}$ multiplied by $Kp_{uu,ss}$ generated using homogenization method in the presence of BSA and temperature method showed the most robust correlation with systemic hepatic CL. Some compounds are equally well predicted by all the approaches tested, regardless of addition of BSA, for example, rosuvastatin,

TABLE 3

$Kp_{,uu}$ values determined in rat hepatocytes using different methods

The data are presented as means of two independent experiments (individual data are given in parentheses) or means ± S.D. of three to five independent experiments.

Compound	Temp $Kp_{uu,ss}$		Hom $Kp_{uu,ss}$		$Kp_{uu,V0}$	
	no BSA	with BSA	no BSA	with BSA	no BSA	with BSA
Rosuvastatin	17.1 (13.5, 20.6)	15.4 ± 4.66	12.6 (14.5, 10.7)	19.0 ± 4.52	54.9 (91.6, 18.2)	37.9 ± 11.4
Pravastatin	11.1 (15.8, 6.43)	4.80 (3.90, 5.69)	2.47 (3.84, 1.10)	2.62 (2.82, 2.42)	7.64 (4.88, 10.4)	30.2 (54.5, 5.97)
Valsartan	21.0 ± 14.6	8.43 (12.9, 3.95)	4.70 ± 1.71	96.5 (104, 89)	29.6 ± 15.9	12.8 (11.1, 14.5)
Pitavastatin	15.1 (22.1, 8.15)	11.6 ± 2.38	4.28 (4.10, 4.46)	7.30 ± 3.55	9.06 (6.22, 11.9)	6.33 ± 0.91
Fluvastatin	5.27 (5.42, 5.12)	20.1 (26.4, 13.7)	4.20 (4.90, 3.50)	16.6 (17.4, 15.8)	4.42 (5.60, 3.24)	11.7 (9.40, 13.9)
Cerivastatin	8.62 ± 1.37	5.75 (6.49, 5.0)	8.00 ± 0.71	15.8 (11.8, 19.7)	7.56 ± 0.33	6.25 ± 5.17
Nateglinide	10.8 (11.1, 10.4)	4.90 (6.80, 2.99)	2.27 (2.37, 2.16)	5.30 (4.85, 5.74)	5.22 (4.41, 6.02)	2.24 (2.09, 2.39)
Atorvastatin	10.5 (9.86, 11.2)	11.2 (10.3, 12.1)	4.71 (3.28, 6.14)	9.08 ± 4.01	12.8 (12.8, 12.7)	10.4 ± 5.36
Bosentan	5.51 (5.14, 5.88)	3.90 (3.53, 4.26)	4.38 (3.20, 5.56)	4.64 ± 1.96	6.31 (5.00, 7.62)	8.72 ± 3.51
Glyburide	6.73 (7.11, 6.35)	17.1 (23.5, 10.6)	2.26 (1.92, 2.60)	16.8 (14.9, 18.6)	19.4 (16.6, 22.2)	94.0 (14.9, 173)
Asunaprevir	5.02 (5.58, 4.45)	10.8 (11.2, 10.4)	0.94 (0.646, 1.24)	1.51 ± 0.11	2.12 (2.67, 1.56)	5.19 (4.24, 6.13)
Telmisartan	2.17 (1.89, 2.45)	4.17 ± 0.72	0.74 (0.647, 0.832)	6.84 ± 1.23	ND (n = 2)	35.6 ± 10.0

ND, not detected.

TABLE 4

Predicted rat hepatic clearance based on the extended clearance concept: $CL_{int,met} \times Kp_{uu}$

Compound	Observed rat CL*a*	$CL_{int,\ met}$	Temp $Kp_{uu,ss}$				Hom $Kp_{uu,ss}$				$Kp_{uu,\ v0}$				
			no BSA		with BSA		no BSA		w BSA		no BSA		w BSA		
		Rat hepatocyte $CL_{int,met}$ *b*	Pred rat CL	CL_{int}	Pred rat CL	CL_{int}	Pred rat CL	CL_{int}	Pred rat CL	CL_{int}	Pred rat CL	CL_{int}	Pred rat CL	CL_{int}	Pred rat CL
	ml/min per kilogram	ml/min per kilogram	ml/min per kilogram	ml/min per kilogram	ml/min per kilogram	ml/min per kilogram	ml/min per kilogram	ml/min per kilogram	ml/min per kilogram	ml/min per kilogram	ml/min per kilogram	ml/min per kilogram	ml/min per kilogram	ml/min per kilogram	ml/min per kilogram
Rosuvastatin	56.7	77.0	5.23	1706	31.7	1541	30.6	1261	28.5	1901	32.7	5493	40.4	3794	38.3
Pravastatin	59.7	28.5*c*	14.51	373	38.6	161	31.7	83	24.5	88	25.2	257	35.9	1015	43.1
Valsartan	17.8	79.2	0.29	2107	5.4	844	2.3	471	1.3	9669	17.4	2962	7.2	1283	3.4
Pitavastatin	28.0	179	1.99	4848	18.7	3733	15.9	1372	7.5	2341	11.4	2904	13.4	2029	10.3
Fluvastatin	20.0	151	4.04	1557	15.5	5925	30.4	1241	13.3	4906	28.4	1306	13.8	3443	24.4
Cerivastatin	24.7	186	7.64	2719	29.1	1813	24.6	2523	28.3	4970	35.0	2385	27.7	1971	25.6
Nateglinide	58.1	169	3.23	2492	20.7	1135	12.4	525	6.7	1228	13.2	1209	13.0	519	6.7
Atorvastatin	35.0	353	14.04	5900	37.9	6275	38.4	2639	31.1	5089	36.9	7143	39.2	5836	37.9
Bosentan	23.0	153	1.98	1280	9.1	905	6.9	1018	7.6	1079	8.0	1466	10.2	2027	13.0
Glyburide	6.8	212	0.70	2375	4.3	6017	9.5	798	1.5	5911	9.4	6846	10.6	33,154	27.2
Asunaprevir	38.4	141	5.24	2280	18.1	4910	26.8	429	5.0	688	7.5	961	9.8	2357	18.4
Telmisartan	14.6	90.6	1.20	437	2.5	840	4.6	149	0.9	1378	7.1	ND	ND	7168	22.5

ND, not detected.

[a]Refer to Table 2.

[b]$CL_{int,\ met}$ (milligrams per minute per kilogram) values was calculated based on the $CL_{int,\ met}$ (microliters per minute per 10^6cells) list in Table 1 using scaling factor of 108×10^6 cells/g liver and 36 g liver/kg body weight.

[c]Determined in rat liver S9 at unit of milliliters per minute per gram liver (Watanabe et al., 2009), converted to milliliters per minute per kilogram using scaling factor of 36 g liver/kg body weight.

fluvastatin, cerivastatin, atorvastatin, and bosentan; the compounds that are sensitive to the IVIVE approaches and the presence of BSA include pravastatin, valsartan, telmisartan, asunaprevir, pitavastatin, nateglinide, and glyburide.

For 8 out of 12 compounds, $PS_{u,inf}$ value determined in the presence of BSA is similar to that in the absence of BSA; two compounds (fluvastatin and glyburide) showed about 3-fold increase of $PS_{u,inf}$ value in the presence of BSA; two compounds (valsartan and telmisartan) demonstrated greater than 10-fold increase in $PS_{u,inf}$ value in the presence of BSA. In contrast, the impact of albumin on the $PS_{u,inf}$ observed in human hepatocytes is more significant (unpublished data from our laboratory and Kim et al., 2019). The increase of unbound intrinsic hepatic uptake in the presence of BSA can be attributed to albumin-mediated hepatic uptake. The "facilitated-dissociation" model has been proposed recently to explain the phenomena where interaction of the albumin-drug complex with the cell surface enhances dissociation

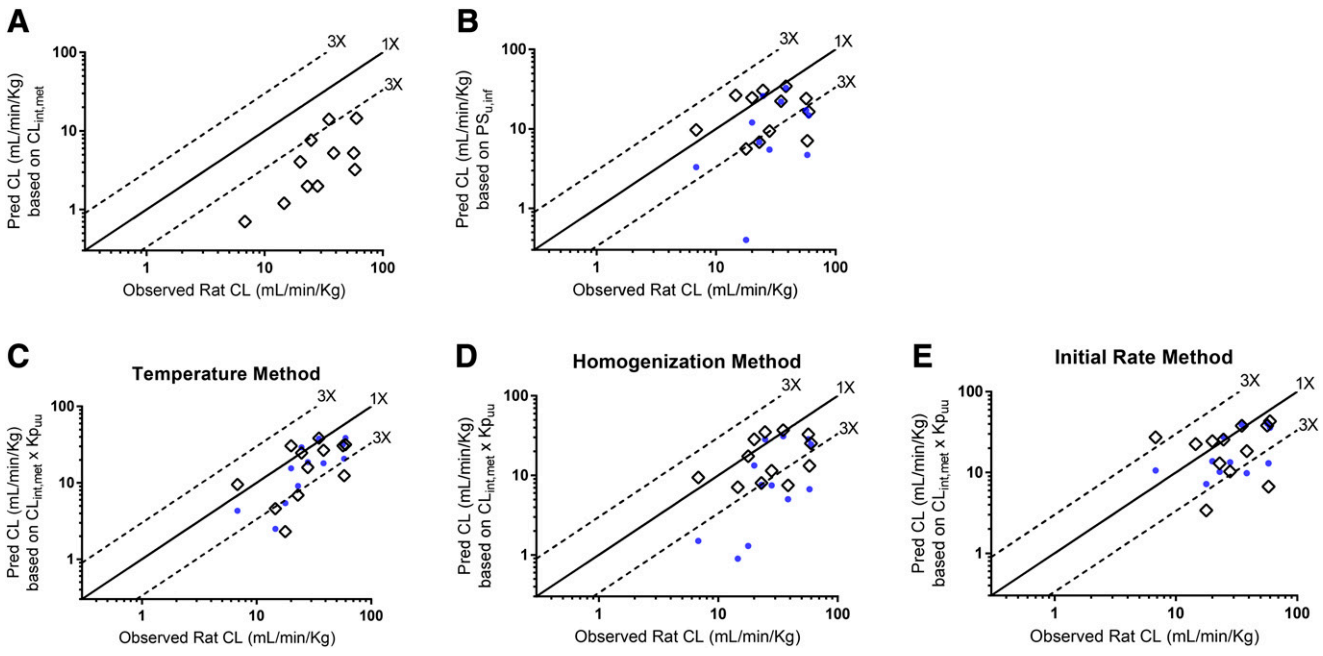

Fig. 2. Correlation of the predicted hepatic CL using different IVIVE approaches with the observed in vivo hepatic CL in rat. Predicted hepatic CL based on intrinsic metabolic CL determined in rat hepatocytes (A). Predicted hepatic CL based on initial hepatic uptake CL determined in rat hepatocytes suspension (B). The open diamond symbol represents the unbound initial uptake CL ($PS_{u,inf}$) determined in KHB containing 4% BSA; the blue circle represents the initial uptake CL ($PS_{u,inf}$) determined in KHB with no BSA. Predicted hepatic CL based upon the extended clearance concept, corrected intrinsic metabolic CL by Kp_{uu} determined using temperature method (C), homogenization method (D), and initial rate method (E). The open diamond symbol represents the Kp_{uu} determined in KHB containing 4% BSA; the blue circle represents the Kp_{uu} determined in the absence of 4% BSA.

TABLE 5

Comparison of the CL predictability by the tested IVIVE approaches (Observed: predicted)

	$CL_{int,met}$	$PS_{u,\ inf}$		Temp $Kp_{uu,ss}$		Hom $Kp_{uu,ss}$		$Kp_{uu,\ v0}$	
		no BSA	w BSA	no BSA	w BSA	no BSA	w BSA	no BSA	w BSA
Rosuvastatin	10.8	3.3	2.3	1.8	1.8	2.0	1.7	1.4	1.5
Pravastatin	4.1	4.0	3.6	1.5	1.9	2.4	2.4	1.7	1.4
Valsartan	61.6	46.9	3.2	3.3	7.7	13.4	1.0	2.5	5.2
Pitavastatin	14.0	5.1	3.0	1.5	1.8	3.7	2.4	2.1	2.7
Fluvastatin	4.9	1.7	1.2	1.3	1.5	1.5	1.4	1.5	1.2
Cerivastatin	3.2	1.1	1.2	1.2	1.0	1.1	1.4	1.1	1.0
Nateglinide	18.0	12.5	8.2	2.8	4.7	8.6	4.4	4.5	8.7
Atorvastatin	2.5	1.6	1.6	1.1	1.1	1.1	1.1	1.1	1.1
Bosentan	11.6	3.4	3.4	2.5	3.4	3.0	2.9	2.3	1.8
Glyburide	9.8	2.0	1.4	1.6	1.4	4.4	1.4	1.6	4.0
Asunaprevir	7.3	1.2	1.1	2.1	1.4	7.7	5.1	3.9	2.1
Telmisartan	12.2	ND	1.8	5.8	3.2	16.4	2.1	ND	1.5
AAFE	8.99	3.48	2.23	1.95	2.11	3.72	2.00	1.92[a]	2.11[a]
RMSLE	0.83,	0.58	0.40	0.32	0.37	0.58	0.35	0.32[a]	0.4[a]

ND, not detected.
[a]Not included the interexperimental variability.

of the complex to present more unbound drug molecules to be transported (Miyauchi et al., 2018; Kim et al., 2019). Another group proposed transporter-induced protein binding shift model, where high affinity binding to transporters may strip ligands off of the plasma protein before they dissociate (Bowman et al., 2019). Based on these theories, the compounds with low binding to albumin should show less change in the $PS_{u,inf}$ in the presence of BSA, whereas addition of BSA should demonstrate higher impact on the compounds with high binding to albumin. However, our data indicated the impact of albumin on the $PS_{u,inf}$ was not always shown for the compounds with high protein binding ($f_{u,p} < 0.01$), i.e., bosentan and pitavastatin. Our finding suggested that the "albumin-mediated" hepatic uptake phenomenon could vary among compounds or between species, which may be attributed to interspecies difference in albumin binding, and expression or function of hepatic uptake transporters between human and rat. The relationship of albumin-mediated transport with variety of molecule properties requires further investigations, i.e., in silico prediction (Liu et al., 2016). It is important to note that there may be difference in protein binding between rat plasma protein and BSA as well. The compound avidly bound to albumin may have strong nonspecific binding to cell surface or assay device due to the high lipophilicity. In the aqueous buffer, the loss of compounds in the nominal concentration could be another reason for underestimation in the in vitro assay. Therefore, it is important to calculate the $PS_{u,inf}$ using experimentally measured medium concentration.

Several in vitro methods have been developed and used to estimate the value of Kp_{uu}. The temperature method refers to $Kp_{uu,ss}$ estimated in hepatocytes using $f_{u,\ liver}$ determined by 1/Kp at 4°C based upon the assumptions that active transport is completely abolished on ice and that tissue binding is not temperature-dependent (Shitara et al., 2013; Riede et al., 2017; Yoshikado et al., 2017). Ryu et al. (2018) have demonstrated that the drug binding properties are not influenced by assay temperature. Our study showed $Kp_{uu,ss}$ estimated using temperature method was not impacted by addition of BSA, and $CL_{int,met}$ corrected by this $Kp_{uu,ss}$ demonstrated the most robust correlation with in vivo observed rat CL, which provide experimental evidence of vitality of these assumptions.

The homogenization method refers to $Kp_{uu,ss}$ determined using experimentally measured $f_{u,\ liver}$ in liver homogenate. The fundamental assumption of this method is that drug binding to the intracellular compartment is not affected by the homogenization process. For the least bound drug, i.e., pravastatin, and the drug with high molecular weight, i.e., asunaprevir, the $Kp_{uu,ss}$ generated using this method was significantly lower compared with other methods. This phenomenon may be associated with the native caveat of the method for measuring the f_u in tissue/cell homogenate (Riede et al., 2017). Mechanical homogenization not only disrupts the plasma membrane but also breaks subcellular organelles, resulting in increased number of intracellular binding sites to the drugs (de Araujo et al., 2015; Keemink et al., 2015). Hence, $f_{u,\ liver}$ for the compounds with less lipophilicity or higher molecular weight can be underestimated. In addition, for the compounds with high binding to plasma, i.e., valsartan, telmisartan, and glyburide, $Kp_{uu,ss}$ estimated using this method was significantly enhanced by supplementing the uptake assay with 4% BSA, subsequently leading to improved hepatic CL prediction, which can be contributed by two factors: 1) albumin-mediated hepatic uptake and/or 2) reduced nonspecific binding of test compounds to the cell surface or assay device.

The initial rate method refers to $Kp_{uu,v0}$ determined from the initial active uptake and passive diffusion (Yabe et al., 2011). Comparatively, the $Kp_{uu,\ ss}$ method has a practical advantage over this method to obtain the $Kp_{uu,\ v0}$ value, as the experimental variability is much less for measuring $Kp_{uu,ss}$ than for $Kp_{uu,\ v0}$, at least in our hands. The uptake data at longer time (15 or 30 minutes, ~ steady state) are enough for $Kp_{uu,ss}$ estimation, whereas initial uptake rates obtained within seconds are required for $Kp_{uu,\ v0}$ determination. Thus, complexity in the assay procedure such a rapid sampling at quick intervals could be a practical limitation of the latter approach. As $Kp_{uu,v0}$ is determined by PS_{inf} and PS_{dif}, the impact of BSA on the $Kp_{uu,\ v0}$ should be aligned with the effect of BSA on PS_{inf}, if PS_{dif} is not influenced by addition of BSA. The large assay variation is mainly attributed to PS_{dif} determined at 37°C with hepatic uptake inhibitor. The phenomenon of albumin-mediated hepatic uptake has only been investigated at the level of total influx. Therefore, the impact of albumin on active uptake versus passive diffusion, and on other uptake (e.g., organic anion transporters) and efflux (e.g., multidrug resistance-associated proteins) transporters would require further investigation.

In conclusion, this study has demonstrated that the hepatic CL mediated by OATP transporter can be predicted reasonably well based upon the extended clearance concept regardless of the involvement of metabolism and lipophilicity of the test compounds. Taking into account the assumptions and practical limitation of all the investigated methods, both intrinsic hepatic uptake CL determined in rat hepatocyte suspension in the presence of 4% BSA, and adjusted $CL_{int,met}$ by hepatocyte to medium unbound concentration ratio determined in rat hepatocytes

suspension at steady state provided robust correlation with the observed in vivo rat hepatic CL without any empirical scaling factor. In light of these findings, this study provided a practical strategy for improved predictions of transporter-mediated hepatic CL to support the optimization of new molecular entities in the early stage of drug discovery. The establishment of IVIVC in preclinical stage will build our confidence in human PK prediction as a necessary step toward the first-in-human study.

Acknowledgments

The authors would like to acknowledge Q^2 Solutions for permeability measurements and Syngene International Limited for rat in vivo PK studies. The authors would also like to thank Dan Rock, Jan Wahlstrom, and Dean Hickman for their support of this work.

Authorship Contributions

Participated in research design: N. Li, Badrinarayanan, Gupta.

Conducted experiments: N. Li, Badrinarayanan, X. Li, Roberts, Hayashi, Virk.

Performed data analysis: N. Li, Badrinarayanan, Gupta.

Wrote or contributed to the writing of the manuscript: N. Li, Badrinarayanan, Roberts, Hayashi, Gupta.

References

Bowman CM, Okochi H, and Benet LZ (2019) The presence of a transporter-induced protein binding shift: a new explanation for protein-facilitated uptake and improvement for in vitro-in vivo extrapolation. *Drug Metab Dispos* **47**:358–363.

de Araújo ME, Lamberti G, and Huber LA (2015) Homogenization of mammalian cells. *Cold Spring Harb Protoc* **2015**:1009–1012.

Di L, Keefer C, Scott DO, Strelevitz TJ, Chang G, Bi YA, Lai Y, Duckworth J, Fenner K, Troutman MD, et al. (2012) Mechanistic insights from comparing intrinsic clearance values between human liver microsomes and hepatocytes to guide drug design. *Eur J Med Chem* **57**: 441–448.

Hallifax D, Foster JA, and Houston JB (2010) Prediction of human metabolic clearance from in vitro systems: retrospective analysis and prospective view. *Pharm Res* **27**:2150–2161.

Hirano M, Maeda K, Shitara Y, and Sugiyama Y (2004) Contribution of OATP2 (OATP1B1) and OATP8 (OATP1B3) to the hepatic uptake of pitavastatin in humans. *J Pharmacol Exp Ther* **311**: 139–146.

Giacomini KM, Huang SM, Tweedie DJ, Benet LZ, Brouwer KL, Chu X, Dahlin A, Evers R, Fischer V, Hillgren KM, et al.; International Transporter Consortium (2010) Membrane transporters in drug development. *Nat Rev Drug Discov* **9**:215–236.

Izumi S, Nozaki Y, Komori T, Takenaka O, Maeda K, Kusuhara H, and Sugiyama Y (2017) Comparison of the predictability of human hepatic clearance for organic anion transporting polypeptide substrate drugs between different in vitro-in vivo extrapolation approaches. *J Pharm Sci* **106**:2678–2687.

Jones HM, Barton HA, Lai Y, Bi YA, Kimoto E, Kempshall S, Tate SC, El-Kattan A, Houston JB, Galetin A, et al. (2012) Mechanistic pharmacokinetic modeling for the prediction of transporter-mediated disposition in humans from sandwich culture human hepatocyte data. *Drug Metab Dispos* **40**:1007–1017.

Kalvass JC, Maurer TS, and Pollack GM (2007) Use of plasma and brain unbound fractions to assess the extent of brain distribution of 34 drugs: comparison of unbound concentration ratios to in vivo p-glycoprotein efflux ratios. *Drug Metab Dispos* **35**:660–666.

Keemink J, Augustijns P, and Annaert P (2015) Unbound ritonavir concentrations in rat and human hepatocytes. *J Pharm Sci* **104**:2378–2387.

Kilford PJ, Stringer R, Sohal B, Houston JB, and Galetin A (2009) Prediction of drug clearance by glucuronidation from in vitro data: use of combined cytochrome P450 and UDP-glucuronosyltransferase cofactors in alamethicin-activated human liver microsomes. *Drug Metab Dispos* **37**:82–89.

Kim SJ, Lee KR, Miyauchi S, and Sugiyama Y (2019) Extrapolation of in vivo hepatic clearance from in vitro uptake clearance by suspended human hepatocytes for anionic drugs with high binding to human albumin: improvement of in vitro-to-in vivo extrapolation by considering the "albumin-mediated" hepatic uptake mechanism on the basis of the "facilitated-dissociation model". *Drug Metab Dispos* **47**:94–103.

Koyanagi T, Yano K, Kim S, Murayama N, Yamazaki H, and Tamai I (2019) In vivo hepatic clearance of lipophilic drugs predicted by in vitro uptake data into cryopreserved hepatocytes suspended in sera of rats, Guinea pigs, monkeys and humans. *Xenobiotica* **49**: 887–894.

Kusuhara H and Sugiyama Y (2009) In vitro-in vivo extrapolation of transporter-mediated clearance in the liver and kidney. *Drug Metab Pharmacokinet* **24**:37–52.

Li R, Barton HA, and Varma MV (2014) Prediction of pharmacokinetics and drug-drug interactions when hepatic transporters are involved. *Clin Pharmacokinet* **53**:659–678.

Liu HC, Goldenberg A, Chen Y, Lun C, Wu W, Bush KT, Balac N, Rodriguez P, Abagyan R, and Nigam SK (2016) Molecular properties of drugs interacting with SLC22 transporters OAT1, OAT3, OCT1, and OCT2: a machine-learning approach. *J Pharmacol Exp Ther* **359**:215–229.

Miyauchi S, Masuda M, Kim SJ, Tanaka Y, Lee KR, Iwakado S, Nemoto M, Sasaki S, Shimono K, Tanaka Y, et al. (2018) The phenomenon of albumin-mediated hepatic uptake of organic anion transport polypeptide substrates: prediction of the in vivo uptake clearance from the in vitro uptake by isolated hepatocytes using a facilitated-dissociation model. *Drug Metab Dispos* **46**: 259–267.

Mosure KW, Knipe JO, Browning M, Arora V, Shu YZ, Phillip T, Mcphee F, Scola P, Balakrishnan A, Soars MG, et al. (2015) Preclinical pharmacokinetics and in vitro metabolism of asunaprevir (BMS-650032), a potent hepatitis C virus NS3 protease inhibitor. *J Pharm Sci* **104**: 2813–2823.

Nakai D, Kumamoto K, Sakikawa C, Kosaka T, and Tokui T (2004) Evaluation of the protein binding ratio of drugs by a micro-scale ultracentrifugation method. *J Pharm Sci* **93**:847–854.

Pang KS and Rowland M (1977) Hepatic clearance of drugs. I. Theoretical considerations of a "well-stirred" model and a "parallel tube" model. Influence of hepatic blood flow, plasma and blood cell binding, and the hepatocellular enzymatic activity on hepatic drug clearance. *J Pharmacokinet Biopharm* **5**:625–653.

Patilea-Vrana G and Unadkat JD (2016) Transport vs. metabolism: what determines the pharmacokinetics and pharmacodynamics of drugs? Insights from the extended clearance model. *Clin Pharmacol Ther* **100**:413–418.

Rabbani G and Ahn SN (2019) Structure, enzymatic activities, glycation and therapeutic potential of human serum albumin: a natural cargo. *Int J Biol Macromol* **123**:979–990.

Riccardi KA, Tess DA, Lin J, Patel R, Ryu S, Atkinson K, Di L, and Li R (2019) A novel unified approach to predict human hepatic clearance for both enzyme- and transporter-mediated mechanisms using suspended human hepatocytes. *Drug Metab Dispos* **47**:484–492.

Riede J, Camenisch G, Huwyler J, and Poller B (2017) Current in vitro methods to determine hepatic Kp_{uu}: a comparison of their usefulness and limitations. *J Pharm Sci* **106**:2805–2814.

Ryu S, Novak JJ, Patel R, Yates P, and Di L (2018) The impact of low temperature on fraction unbound for plasma and tissue. *Biopharm Drug Dispos* **39**:437–442.

Shitara Y, Horie T, and Sugiyama Y (2006) Transporters as a determinant of drug clearance and tissue distribution. *Eur J Pharm Sci* **27**:425–446.

Shitara Y, Maeda K, Ikejiri K, Yoshida K, Horie T, and Sugiyama Y (2013) Clinical significance of organic anion transporting polypeptides (OATPs) in drug disposition: their roles in hepatic clearance and intestinal absorption. *Biopharm Drug Dispos* **34**:45–78.

Sirianni GL and Pang KS (1997) Organ clearance concepts: new perspectives on old principles. *J Pharmacokinet Biopharm* **25**:449–470.

Tamura M, Shiba S, Kudo N, and Kawashima Y (2010) Pharmacokinetics of nateglinide enantiomers and their metabolites in Goto-Kakizaki rats, a model for type 2 diabetes mellitus. *Chirality* **22**:92–98.

Tessari P (2003) Protein metabolism in liver cirrhosis: from albumin to muscle myofibrils. *Curr Opin Clin Nutr Metab Care* **6**:79–85.

Treiber A, Schneiter R, Delahaye S, and Clozel M (2004) Inhibition of organic anion transporting polypeptide-mediated hepatic uptake is the major determinant in the pharmacokinetic interaction between bosentan and cyclosporin A in the rat. *J Pharmacol Exp Ther* **308**:1121–1129.

Tsao SC, Sugiyama Y, Sawada Y, Iga T, and Hanano M (1988a) Kinetic analysis of albumin-mediated uptake of warfarin by perfused rat liver. *J Pharmacokinet Biopharm* **16**:165–181.

Tsao SC, Sugiyama Y, Shinmura K, Sawada Y, Nagase S, Iga T, and Hanano M (1988b) Protein-mediated hepatic uptake of rose bengal in analbuminemic mutant rats (NAR). Albumin is not indispensable to the protein-mediated transport of rose bengal. *Drug Metab Dispos* **16**:482–489.

Watanabe T, Kusuhara H, Maeda K, Kanamaru H, Saito Y, Hu Z, and Sugiyama Y (2010) Investigation of the rate-determining process in the hepatic elimination of HMG-CoA reductase inhibitors in rats and humans. *Drug Metab Dispos* **38**:215–222.

Watanabe T, Kusuhara H, Maeda K, Shitara Y, and Sugiyama Y (2009) Physiologically based pharmacokinetic modeling to predict transporter-mediated clearance and distribution of pravastatin in humans. *J Pharmacol Exp Ther* **328**:652–662.

Watanabe T, Kusuhara H, Watanabe T, Debori Y, Maeda K, Kondo T, Nakayama H, Horita S, Ogilvie BW, Parkinson A, et al. (2011) Prediction of the overall renal tubular secretion and hepatic clearance of anionic drugs and a renal drug-drug interaction involving organic anion transporter 3 in humans by in vitro uptake experiments. *Drug Metab Dispos* **39**:1031–1038.

Wienen W, Entzeroth M, van Meel JCA, Stangier J, Busch U, Ebner T, Schmid J, Lehmann H, Matzek K, Kempthorne-Rawson J, et al. (2000) A review on telmisartan: a novel, long-acting angiotensin II-receptor antagonist. *Cardiovasc Drug Rev* **18**:127–154.

Yabe Y, Galetin A, and Houston JB (2011) Kinetic characterization of rat hepatic uptake of 16 actively transported drugs. *Drug Metab Dispos* **39**:1808–1814.

Yamashiro W, Maeda K, Hirouchi M, Adachi Y, Hu Z, and Sugiyama Y (2006) Involvement of transporters in the hepatic uptake and biliary excretion of valsartan, a selective antagonist of the angiotensin II AT1-receptor, in humans. *Drug Metab Dispos* **34**:1247–1254.

Yoshikado T, Toshimoto K, Nakada T, Ikejiri K, Kusuhara H, Maeda K, and Sugiyama Y (2017) Comparison of methods for estimating unbound intracellular-to-medium concentration ratios in rat and human hepatocytes using statins. *Drug Metab Dispos* **45**:779–789.

Zhou X, Rougée LR, Bedwell DW, Cramer JW, Mohutsky MA, Calvert NA, Moulton RD, Cassidy KC, Yumibe NP, Adams LA, et al. (2016) Difference in the pharmacokinetics and hepatic metabolism of antidiabetic drugs in zucker diabetic fatty and sprague-dawley rats. *Drug Metab Dispos* **44**:1184–1192.

Address correspondence to: Anshul Gupta, Department of Pharmacokinetics and Drug Metabolism, Amgen Research, Amgen Inc., 360 Binney St., Cambridge, MA 02142. E-mail: agupta.pharmaceuticals@gmail.com

#DMD-AR-2020-000064

Comparison of In Vitro to In Vivo Extrapolation Approaches for Predicting Transporter-Mediated Hepatic Uptake Clearance Using Suspended Rat Hepatocytes

Na Li, Akshay Badrinarayanan, Xingwen Li, John Roberts, Mike Hayashi, Manpreet Virk,

Anshul Gupta*

Department of Pharmacokinetics and Drug Metabolism, Amgen Research, Amgen Inc. Cambridge, MA 02142

*Corresponding Author: Anshul Gupta

Address: Department of Pharmacokinetics and Drug Metabolism, Amgen Research, Amgen Inc.

360 Binney St., Cambridge, MA 02142

Phone: +1 (617) 444 5205

Email: agupta.pharmaceuticals@gmail.com

Journal: Drug Metabolism and Disposition

The material includes Supplemental Table S1, Supplemental Methods and References.

Supplemental Materials:

Table S1: Summary of the in vitro and in vivo evidence of OATP-mediated hepatic uptake of the selected compounds

	Transporters involved in hepatic uptake			Preclinical and clinical evidence of OATP involvement		
Compound	**Approach**	**Hepatic Transporters**	**Reference**	**Approach**	**PK Change**	**Reference**
Rosuvastatin	RAF and REF	OATP1B1 (M) and OATP1B3 (total 96% and 80%)	(Kunze et al., 2014) [a]	oatp1a/1b KO mice	i.v. : AUC↑ 1.7-fold PO: Cmax ↑ 3-fold; AUC↑ 7.1-fold	(Iusuf et al., 2013)
	RAF	OATP1B1(>95%) and OATP1B3 (<5%)	(Izumi et al., 2018) [b]	oatp1a/1b KO mice	i.v. : AUC↑ 2.3-fold PO: Cmax ↑ 35-fold; AUC↑ 48-fold	(Salphati et al., 2014)
	Hepatocytes with inhibitor	OATP1B1/1B3 (71%), 2B1 (21%) and NTCP (6%)	(Bi et al., 2019)	Clinical DDI with rifampicin (RIF)	+ 600 mg RIF: Cmax ↑ 5.2-fold; AUC↑ 2.5-fold	(Mori et al., 2020)
Pravastatin	RAF and REF	OATP1B1 (M) and OATP1B3 (total 88% and 70%)	(Kunze et al., 2014) [a]	oatp1a/1b KO mice	AUC↑ 4.3-fold	(Higgins et al., 2014)
	RAF	OATP1B1 (>95%) and OATP1B3 (<5%)	(Izumi et al., 2018) [b]	oatp1a/1b KO mice	i.v. AUC↑ 4-fold PO: Cmax ↑ 9.7-fold; AUC↑ 18-fold	(Salphati et al., 2014)
	Hepatocytes with inhibitor	OATP1B1/1B3 (98%)	(Bi et al., 2019)	Clinical DDI with cyclosporin A (CsA)	+ 2x 100 mg CsA: Cmax ↑ 3.2-fold; AUC↑ 3.4-fold	(Yee et al., 2019)
Valsartan	RAF	OATP1B1 (20-70%) and 1B3 (30-80%)	(Yamashiro et al., 2006)	Clinical DDI with RIF	+ 600 mg RIF: Cmax ↑ 3.7-fold; AUC↑ 5.5-fold	(Mori et al., 2020)
	RAF	OATP1B1 (>75%) and 1B3 (<25%)	(Izumi et al., 2018)[b]			
Pitavastatin	RAF	OATP1B1 (90%) and OATP1B3 (10%)	(Hirano et al., 2004)	oatp1a/1b KO mice	PO: Cmax ↑ 13.5-fold; AUC↑ 11.7-fold	(Salphati et al., 2014)
	RAF and REF	OATP1B1 (M) and OATP1B3 (total 43% and 35%)	(Kunze et al., 2014) [a]	oatp1a/1b KO mice	i.v.: AUC↑ 3.7-fold	(Chang et al., 2019)
	RAF	OATP1B1 (>90%) and OATP1B3 (<10%)	(Izumi et al., 2018) [b]	Clinical DDI with RIF	+ 600 mg RIF: Cmax ↑ 3.7-fold; AUC↑ 4.0-fold	(Mori et al., 2020)
	Hepatocytes: inhibitor	OATP1B1/1B3 (81%), 2B1 (12%)	(Bi et al., 2019)			
Fluvastatin	RAF and REF	OATP1B1 (M) and OATP1B3 (total 50% and 42%)	(Kunze et al., 2014) [a]	oatp1a/1b KO mice	i.v.: AUC↑ 1.7-fold	(Chang et al., 2019)
	RAF	OATP1B1 (>93%) and OATP1B3 (<7%)	(Izumi et al., 2018) [b]			
	Hepatocytes: inhibitor	OATP1B1/1B3 (48%), 2B1 (12%) and NTCP (16%)	(Bi et al., 2019)			
Cerivastatin	RAF and REF	OATP1B1 (M) and OATP1B3 (total 19% and 16%)	(Kunze et al., 2014) [a]	Clinical DDI with CsA	AUC↑ 3.8-fold	(Shitara et al., 2013)
	RAF	OATP1B1 (>95%) and OATP1B3 (<5%)	(Izumi et al., 2018) [b]			
Nateglinide	RAF	OATP1B1(>85%) and 1B3 (<15%)	(Izumi et al., 2018) [b]	Clinical DDI with fluconazole	AUC↑ 1.5-fold	(Niemi et al., 2003)
Atorvastatin	RAF and REF	OATP1B1 (M) and OATP1B3 (total 73% and 63%)	(Kunze et al., 2014) [a]	oatp1a/1b KO mice	AUC↑ 19-fold	(Higgins et al., 2014)
	RAF	OATP1B1 (>85%) and 1B3(<15%)	(Izumi et al., 2018) [b]	Clinical DDI with RIF	+ 600 mg RIF: Cmax ↑ 13.3-fold; AUC↑ 7.3-fold	(Mori et al., 2020)
Bosentan	RAF	OATP1B1 (>90%) and 1B3 (<10%)	(Izumi et al., 2018) [b]	Clinical DDI with RIF	+ 600 mg RIF: AUC↑ 3.2-fold	(Yoshikado et al., 2017)
Glyburide	RAF	OATP1B1 (>95%) and 1B3 (<5%)	(Izumi et al., 2018) [b]	Clinical DDI with RIF	+ 600 mg RIF: AUC↑ 2.2-fold	(Shitara et al., 2013)
Asunaprevir	Hepatocytes	Saturable Uptake	(Eley et al., 2015)	Clinical DDI with rifampin	PO: Cmax ↑ 21-fold; AUC↑ 15-fold	(Eley et al., 2015)
Telmisartan	RAF	OATP1B3 only	(Ishiguro et al., 2006)	Clinical DDI with Nisoldipine	AUC↑ 2.3-fold	(Bajcetic et al., 2007)
	RAF	OATP1B3 only	(Izumi et al., 2018) [b]			

[a]In Kunze, et al, the percent contribution of both OATP1B1 and OATP1B3 to the total active hepatic uptake clearance determined using RAF and REF respectively were listed in the parentheses. M in the parentheses indicated the major OATP involved in hepatic uptake.

[b]The percent contribution (%) cited from Izumi, et al and others represents the relative contribution of OATP1B1 and OATP1B3 to hepatic uptake.

RIF: rifampicin

CsA: cyclosporin A

Supplemental methods:

Bioanalysis using RapidFire

Analysis of specimens for intrinsic metabolic CL in rat hepatocytes was performed using the RapidFire 365 high-throughput SPE system interfaced with a 6550 QTOF mass spectrometer with dual Agilent Jet (AJS) ESI source (Agilent Technologies, Santa Clara, CA, USA). The instrument settings were gas temperature at 200°C, drying gas at 18 l/min, nebulizer 40 psig, sheath gas temperature at 350°C, sheath gas flow at 12 l/min and Vcap at 5000 V. The acquisition rate/time was 5 spectra/s and Mass range was 100 to 700 m/z. Specimens were analyzed in positive mode. The load/wash solvent (solvent A) was water containing 0.1% (v/v) formic acid. The elution solvent (solvent B) was acetonitrile containing 0.1% (v/v) formic acid. Specimens were aspirated serially, under vacuum, directly from multi-well assay plates. In each case, a 10 µL aliquot was loaded onto a C18 SPE cartridge (cartridge type A) to remove buffer salts, using solvent A at a flow rate of 1.5 ml/min for 3500 ms. The retained and purified analytes were eluted to the mass spectrometer by washing the cartridge with solvent B at 0.60 to 0.8 ml/min for 3500 ms. The cartridge was re-equilibrated with solvent A for 500 ms at 1.5 ml/min. The entire sampling cycle was around 8 s per well, enabling the analysis of a 96-well plate in approximately 13 min.

LC-MS/MS Quantification

The Shimadzu LC system included two LC-20ADXR pumps, a SIL-30ACMP auto sampler, a CBM-20A controller and a CTO-20A column oven (Shimadzu, USA). The chromatography was performed using C18 column (Cadenza 5CD - C18, 5 µM, 2 X 30mm, Imtakt, USA). Sample injection volume was 5µL and the LC flow rate was 1.2 mL/min. Mobile phase (A) was water with 0.1% formic acid and mobile phase (B) was acetonitrile with 0.1% formic acid. The gradient elution started with a 0.1 min hold at 5% mobile phase (B), followed by a 0.8 min ramp to 95% mobile phase (B) and hold for 0.5 min, followed by a 0.1 min ramp to 5% mobile phase (B) and a hold for 0.4 min re-equilibration. Integrated valco valve was used and the injected liquid was directed into Mass Spectrometer from 0.3 min to 1.8 min. The triple-quadruple instrument is an AB Sciex 5500 QTrap. The mass spectrometer and peripherals were all controlled by Analyst™ (version 1.6.3; AB Sciex, Ontario, Canada) and DiscoveryQuant™

software (version 3.0.1; AB Sciex, Ontario, Canada). Positive ionizations were used in selected reaction monitoring (MRM) scan mode. All the transitions of twelve compounds are listed below.

Compound	MW	Q1	Q3	DP	CE	CPX	EP
Glyburide	494	495.2	370.1	73	10	9	8
Nateglinide	317	318.2	69.1	120	25	13	12
Valsartan	435	436.2	291.1	43	10	13	12
Telmisartan	514	515.0	276.1	162	50	13	2
Atorvastatin	558	559.4	440.3	81	10	16	10
Asunaprevir	747	748.3	648.3	60	27	17	5
Pitavastatin	421	422.5	290.2	96	39	10	10
Bosentan	551	551.8	202.0	154	25	15	2
Rosuvastatin	481	482.0	258.1	76	28	20	10
Cerivastatin	459	460.2	356.3	86	20	12	10
Fluvastatin	411	412.3	224.1	71	30	22	10
Pravastatin	446	447.1	327.4	50	23	30	10

References

Bajcetic M, Benndorf RA, Appel D, Schwedhelm E, Schulze F, Riekhof D, Maas R and Boger RH (2007) Pharmacokinetics of oral doses of telmisartan and nisoldipine, given alone and in combination, in patients with essential hypertension. *J Clin Pharmacol* **47**:295-304.

Bi YA, Costales C, Mathialagan S, West M, Eatemadpour S, Lazzaro S, Tylaska L, Scialis R, Zhang H, Umland J, Kimoto E, Tess DA, Feng B, Tremaine LM, Varma MVS and Rodrigues AD (2019) Quantitative Contribution of Six Major Transporters to the Hepatic Uptake of Drugs: "SLC-Phenotyping" Using Primary Human Hepatocytes. *J Pharmacol Exp Ther* **370**:72-83.

Chang JH, Zhang X, Messick K, Chen YC, Chen E, Cheong J and Ly J (2019) Unremarkable impact of Oatp inhibition on the liver concentration of fluvastatin, lovastatin and pitavastatin in wild-type and Oatp1a/1b knockout mouse. *Xenobiotica* **49**:602-610.

Eley T, Han YH, Huang SP, He B, Li W, Bedford W, Stonier M, Gardiner D, Sims K, Rodrigues AD and Bertz RJ (2015) Organic anion transporting polypeptide-mediated transport of, and inhibition by, asunaprevir, an inhibitor of hepatitis C virus NS3 protease. *Clin Pharmacol Ther* **97**:159-166.

Higgins JW, Bao JQ, Ke AB, Manro JR, Fallon JK, Smith PC and Zamek-Gliszczynski MJ (2014) Utility of Oatp1a/1b-knockout and OATP1B1/3-humanized mice in the study of OATP-mediated pharmacokinetics and tissue distribution: case studies with pravastatin, atorvastatin, simvastatin, and carboxydichlorofluorescein. *Drug Metab Dispos* **42**:182-192.

Hirano M, Maeda K, Shitara Y and Sugiyama Y (2004) Contribution of OATP2 (OATP1B1) and OATP8 (OATP1B3) to the hepatic uptake of pitavastatin in humans. *J Pharmacol Exp Ther* **311**:139-146.

Ishiguro N, Maeda K, Kishimoto W, Saito A, Harada A, Ebner T, Roth W, Igarashi T and Sugiyama Y (2006) Predominant contribution of OATP1B3 to the hepatic uptake of telmisartan, an angiotensin II receptor antagonist, in humans. *Drug Metab Dispos* **34**:1109-1115.

Iusuf D, van Esch A, Hobbs M, Taylor M, Kenworthy KE, van de Steeg E, Wagenaar E and Schinkel AH (2013) Murine Oatp1a/1b uptake transporters control rosuvastatin systemic exposure without affecting its apparent liver exposure. *Mol Pharmacol* **83**:919-929.

Izumi S, Nozaki Y, Kusuhara H, Hotta K, Mochizuki T, Komori T, Maeda K and Sugiyama Y (2018) Relative Activity Factor (RAF)-Based Scaling of Uptake Clearance Mediated by Organic Anion Transporting Polypeptide (OATP) 1B1 and OATP1B3 in Human Hepatocytes. *Mol Pharm* **15**:2277-2288.

Kunze A, Huwyler J, Camenisch G and Poller B (2014) Prediction of organic anion-transporting polypeptide 1B1- and 1B3-mediated hepatic uptake of statins based on transporter protein expression and activity data. *Drug Metab Dispos* **42**:1514-1521.

Mori D, Kimoto E, Rago B, Kondo Y, King-Ahmad A, Ramanathan R, Wood LS, Johnson JG, Le VH, Vourvahis M, David Rodrigues A, Muto C, Furihata K, Sugiyama Y and Kusuhara H (2020) Dose-Dependent Inhibition of OATP1B by Rifampicin in Healthy Volunteers: Comprehensive Evaluation of Candidate Biomarkers and OATP1B Probe Drugs. *Clin Pharmacol Ther* **107**:1004-1013.

Niemi M, Neuvonen M, Juntti-Patinen L, Backman JT and Neuvonen PJ (2003) Effect of fluconazole on the pharmacokinetics and pharmacodynamics of nateglinide. *Clin Pharmacol Ther* **74**:25-31.

Salphati L, Chu X, Chen L, Prasad B, Dallas S, Evers R, Mamaril-Fishman D, Geier EG, Kehler J, Kunta J, Mezler M, Laplanche L, Pang J, Rode A, Soars MG, Unadkat JD, van Waterschoot RA, Yabut J, Schinkel AH and Scheer N (2014) Evaluation of organic anion transporting polypeptide 1B1 and 1B3 humanized mice as a translational model to study the pharmacokinetics of statins. *Drug Metab Dispos* **42**:1301-1313.

Shitara Y, Maeda K, Ikejiri K, Yoshida K, Horie T and Sugiyama Y (2013) Clinical significance of organic anion transporting polypeptides (OATPs) in drug disposition: their roles in hepatic clearance and intestinal absorption. *Biopharm Drug Dispos* **34**:45-78.

Yamashiro W, Maeda K, Hirouchi M, Adachi Y, Hu Z and Sugiyama Y (2006) Involvement of transporters in the hepatic uptake and biliary excretion of valsartan, a selective antagonist of the angiotensin II AT1-receptor, in humans. *Drug Metab Dispos* **34**:1247-1254.

Yee SW, Giacomini MM, Shen H, Humphreys WG, Horng H, Brian W, Lai Y, Kroetz DL and Giacomini KM (2019) Organic Anion Transporter Polypeptide 1B1 Polymorphism Modulates the Extent of Drug-Drug Interaction and Associated Biomarker Levels in Healthy Volunteers. *Clin Transl Sci* **12**:388-399.

Yoshikado T, Maeda K, Furihata S, Terashima H, Nakayama T, Ishigame K, Tsunemoto K, Kusuhara H, Furihata KI and Sugiyama Y (2017) A Clinical Cassette Dosing Study for Evaluating the Contribution of Hepatic OATPs and CYP3A to Drug-Drug Interactions. *Pharm Res* **34**:1570-1583.